REPORT DOCUMENTATION PAGE

Form Approved OMB NO. 0704-0188

1. REPORT DATE (DD-MM-YYYY)	2. REPORT TYPE	3. DATES COVERED (From - To)
	New Reprint	-

4. TITLE AND SUBTITLE

Adsorption of 2-Chloroethyl Ethyl Sulfide on Silica: Binding Mechanism and Energy of a Bifunctional Hydrogen-Bond Acceptor at the Gas–Surface Interface

5a. CONTRACT NUMBER
W911NF-09-1-0150

5b. GRANT NUMBER

5c. PROGRAM ELEMENT NUMBER
611102

6. AUTHORS

Joshua Abelard, Amanda R. Wilmsmeyer, Angela C. Edwards, Wesley O. Gordon, Erin M. Durke, Christopher J. Karwacki, Diego Troya, John R. Morris

5d. PROJECT NUMBER

5e. TASK NUMBER

5f. WORK UNIT NUMBER

7. PERFORMING ORGANIZATION NAMES AND ADDRESSES

Virginia Polytechnic Institute & State Unive
North End Center, Suite 4200
300 Turner Street, NW
Blacksburg, VA 24061 -0001

8. PERFORMING ORGANIZATION REPORT NUMBER

9. SPONSORING/MONITORING AGENCY NAME(S) AND ADDRESS (ES)

U.S. Army Research Office
P.O. Box 12211
Research Triangle Park, NC 27709-2211

10. SPONSOR/MONITOR'S ACRONYM(S)
ARO

11. SPONSOR/MONITOR'S REPORT NUMBER(S)
55374-CH.20

12. DISTRIBUTION AVAILIBILITY STATEMENT

Approved for public release; distribution is unlimited.

13. SUPPLEMENTARY NOTES

The views, opinions and/or findings contained in this report are those of the author(s) and should not contrued as an official Department of the Army position, policy or decision, unless so designated by other documentation.

14. ABSTRACT

This work investigates the fundamental nature of sulfur mustard surface adsorption by characterizing interfacial hydrogen bonding and other intermolecular forces for the surrogate molecule (simulant) 2-chloroethyl ethyl sulfide (2-CEES). Adsorption at the surface of amorphous silica is the focus of this work because of silica's low chemical reactivity, well-known properties, and abundance in the environment. 2-CEES has two polar functional groups, the chloro and thioether moieties, available to accept hydrogen bonds from free surface silanol groups. Diethyl sulfide and chlorobutane are also investigated to independently assess the role of the chloro and thioether functionalities in

15. SUBJECT TERMS

CWA, HD, Mustard, Silica, 2-CEES, Adsorption, hydrogen bond

16. SECURITY CLASSIFICATION OF:			17. LIMITATION OF ABSTRACT	15. NUMBER OF PAGES	19a. NAME OF RESPONSIBLE PERSON
a. REPORT	b. ABSTRACT	c. THIS PAGE			John Morris
UU	UU	UU	UU		19b. TELEPHONE NUMBER: 540-231-2472

Report Title

Adsorption of 2-Chloroethyl Ethyl Sulfide on Silica: Binding Mechanism and Energy of a Bifunctional Hydrogen-Bond Acceptor at the Gas–Surface Interface

ABSTRACT

This work investigates the fundamental nature of sulfur mustard surface adsorption by characterizing interfacial hydrogen bonding and other intermolecular forces for the surrogate molecule (simulant) 2-chloroethyl ethyl sulfide (2-CEES). Adsorption at the surface of amorphous silica is the focus of this work because of silica's low chemical reactivity, well-known properties, and abundance in the environment. 2-CEES has two polar functional groups, the chloro and thioether moieties, available to accept hydrogen bonds from free surface silanol groups. Diethyl sulfide and chlorobutane are also investigated to independently assess the role of the chloro and thioester functionalities in the overall adsorption mechanism and to explore the interplay between the charge transfer and electrostatic contributions to total hydrogen-bond strength. Our approach utilizes infrared spectroscopy to study specific surface–molecule interactions and temperature-programmed desorption to measure the activation energy for desorption of adsorbed molecules. Our results indicate that 2-CEES adsorbs to silica by hydrogen bonding through either the chloro or thioether moieties but is unable to form a more stable configuration in which both polar groups interact simultaneously with adjacent silanol groups. The activation energy for desorption of 2-CEES is nearly 43 kJ/mol, driven by both strong hydrogen bonding and other non-bonding interactions. A systematic study of chloroalkanes reveals that each methylene group contributes approximately 5–8 kJ/mol to the overall desorption energy.

REPORT DOCUMENTATION PAGE (SF298)
(Continuation Sheet)

Continuation for Block 13

ARO Report Number 55374.20-CH
Adsorption of 2-Chloroethyl Ethyl Sulfide on Silic...

Block 13: Supplementary Note

Approved for public release; distribution is unlimited.

THE JOURNAL OF PHYSICAL CHEMISTRY C

Article

pubs.acs.org/JPCC

Adsorption of 2-Chloroethyl Ethyl Sulfide on Silica: Binding Mechanism and Energy of a Bifunctional Hydrogen-Bond Acceptor at the Gas−Surface Interface

Joshua Abelard,[†] Amanda R. Wilmsmeyer,[‡] Angela C. Edwards,[†] Wesley O. Gordon,[§] Erin M. Durke,[⊥] Christopher J. Karwacki,[∥] Diego Troya,[†] and John R. Morris*[,†]

[†]Department of Chemistry, Virginia Tech, Blacksburg, Virginia 24061, United States

[‡]Department of Chemistry, Augustana College, Rock Island, Illinois 61201, United States

[§]CBR Filtration Branch and [∥]CB Protection and Decontamination Division, Edgewood Chemical Biological Center, Gunpowder, Maryland 21010, United States

[⊥]Excet, Inc., Springfield, Virginia 22151, United States

ABSTRACT: This work investigates the fundamental nature of sulfur mustard surface adsorption by characterizing interfacial hydrogen bonding and other intermolecular forces for the surrogate molecule (simulant) 2-chloroethyl ethyl sulfide (2-CEES). Adsorption at the surface of amorphous silica is the focus of this work because of silica's low chemical reactivity, well-known properties, and abundance in the environment. 2-CEES has two polar functional groups, the chloro and thioether moieties, available to accept hydrogen bonds from free surface silanol groups. Diethyl sulfide and chlorobutane are also investigated to independently assess the role of the chloro and thioester functionalities in the overall adsorption mechanism and to explore the interplay between the charge transfer and electrostatic contributions to total hydrogen-bond strength. Our approach utilizes infrared spectroscopy to study specific surface−molecule interactions and temperature-programmed desorption to measure the activation energy for desorption of adsorbed molecules. Our results indicate that 2-CEES adsorbs to silica by hydrogen bonding through either the chloro or thioether moieties but is unable to form a more stable configuration in which both polar groups interact simultaneously with adjacent silanol groups. The activation energy for desorption of 2-CEES is nearly 43 kJ/mol, driven by both strong hydrogen bonding and other non-bonding interactions. A systematic study of chloroalkanes reveals that each methylene group contributes approximately 5−8 kJ/mol to the overall desorption energy.

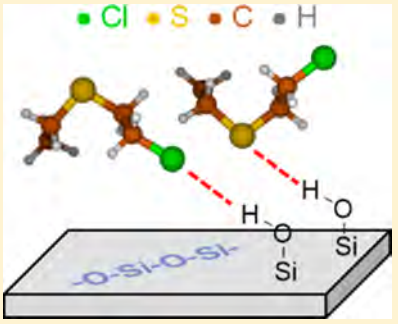

1. INTRODUCTION

Sulfur mustard [bis(2-chloroethyl) sulfide, HD] is an extremely toxic compound that saw widespread use in the First World War as a vesicant chemical warfare agent (CWA).[1] Although the Chemical Weapons Convention (CWC) in 1997 mandated the destruction of mustard stockpiles worldwide, HD can be readily synthesized by terrorists or militaries who choose to ignore the CWC policies.[2] Furthermore, HD is known to be persistent in the environment and can remain at sufficiently high concentrations to pose serious health risks several years after initial deployment.[3] Motivated by this threat, researchers have directed significant effort toward the design of effective protection strategies including sorbent materials, decontamination procedures, and sensors. These technologies often rely on molecule−surface interactions or reactions that are tailored to achieve a particular outcome. However, surprisingly little is known about the fundamental nature of the surface chemistry of sulfur mustard.

As HD, a moderate vapor pressure liquid at room temperature, interacts with the surface of a material, it may accommodate to the surface prior to desorption, diffuse into the bulk of a porous material, or undergo a chemical transformation. The pathways that govern a particular HD−surface interaction are governed in large part by the initial binding energy of the molecule, which controls the molecular residence time on the surface. For molecules like HD that have multiple functional groups with available lone pairs of electrons, one of the most likely initial binding pathways is through the formation of hydrogen bonds with surface hydroxyl groups. For example, interfacial hydrogen bonding has been shown to be the critical first step in the decomposition of 2-chloroethyl ethyl sulfide (2-CEES or "half-mustard") on the surface of a hydroxylated SiO_2−TiO_2 composite nanomaterial.[4,5] Furthermore, surface hydroxyl groups are ubiquitous in nearly any environment, as they decorate the surface of metals, metal oxides, and organic materials. Therefore, the primary focus of the work described below is to provide fundamental insight into the strength and structure of HD−surface hydrogen-bonding interactions through the systematic study of key mimics of the actual chemical warfare agent.

Received: September 19, 2014
Revised: November 19, 2014
Published: November 19, 2014

DOI: 10.1021/jp509516x
J. Phys. Chem. C 2015, 119, 365−372

Research on CWAs typically employs simulants, which are intended to mimic the chemical properties of the live agent without the risk of exposing laboratory personnel to extremely toxic compounds. The most common simulant for HD is the commercially available compound 2-CEES. HD and 2-CEES are structurally nearly identical and differ only by an additional terminal chloro functional group in HD.

Hydrogen-bonding interactions between 2-CEES and the free hydroxyl groups on the surface of a mixed TiO_2−SiO_2 composite material have been previously explored through infrared spectroscopy.[4−7] In those studies, the IR absorptivity of isolated SiO−H stretches on the surface was monitored during 2-CEES adsorption. The data revealed that the SiO−H band underwent extensive changes, indicative of hydrogen-bond formation with both the Cl and S moieties of the adsorbate. The three key changes in the SiO−H band included a shift to lower frequencies, a broadening of the band, and an increase in the absorptivity of the band. Interestingly, the previous work demonstrated that the magnitude of each effect was significantly different for hydrogen bonding through the Cl or the S groups. This effect was ascribed to differences in the electronic structure of the moieties, the result of differing degrees of hybridization in the lone-pair electrons of the hydrogen-bond acceptor. One might then speculate that these differences may also affect the strength of the hydrogen bonds.

Although the hydrogen-bonding energy between a 2-CEES or HD molecule and hydroxyl-containing compounds or surfaces has not yet been (to the best of our knowledge) reported in the literature, several recent studies have focused on the energetic and mechanistic details of hydrogen bonding for similar compounds in the gas phase.[8,9] The understanding that has emerged from those studies is that the character of a hydrogen bond, including its strength, bond length, and spectroscopic signatures, is highly dependent on both electrostatic interactions and the extent of charge transfer between a nonbonding orbital of the acceptor and an antibonding orbital of the hydride donor.[9] For example, a comprehensive computational study[8] of hydrogen-bonding interactions at the ωB97X-D/aug-cc-pVTZ level of theory showed that the OH stretching frequency for the hydrogen-bond donor in H_2O shifts by 88 cm^{-1} when it forms a bond with the chloro group of methyl chloride. However, the OH stretching frequency shifts by more than 200 cm^{-1} when water forms a hydrogen bond with the S moiety of dimethyl sulfide. Despite the large differences in the OH stretching frequency for these two hydrogen bonds, the calculated energies of the bonds differ by only 2 kcal/mol.[8] These computational investigations suggest that hydrogen-bond formation through both the Cl and S groups of 2-CEES (and HD) may contribute significantly to the energetics of adsorption on hydroxyl-containing surfaces.

The work presented here investigates the energy and mechanism of hydrogen-bond formation between 2-CEES, as well as a series of key test molecules, and the surface of silica. Silica was chosen for this work not only because it is one of the most abundant materials found in environmental and industrial settings but also because it can serve as an effective model substrate with well-characterized interfacial hydroxyl groups that can be prepared in a highly reproducible manner. In these studies, transmission infrared spectroscopic measurements are used to probe changes to the vibrational frequency of SiO−H stretches during gas uptake and hydrogen-bond formation. Shifts in this band provide insight into the extent of charge transfer into the antibonding orbital of the hydroxyl group upon the formation of the hydrogen bond. However, the binding energy depends on a complex interplay between charge transfer, electrostatic forces, and other intermolecular forces that cannot be predicted from spectroscopic measurements alone. Therefore, we employ temperature-programmed desorption (TPD) methods to interrogate the activation energy for bond breaking and desorption, which provides insight into the strength of the hydrogen bond. Performing these studies under ultrahigh vacuum (UHV) conditions ensures that the silica surface remains free from contamination throughout the experiment. Overall, these studies provide fundamental insight into hydrogen bonding and the interactions at the gas−surface interface that are responsible for HD uptake, residence time, and, ultimately, surface reactivity.

2. EXPERIMENTAL SECTION

Instrumentation. The instrumentation and general procedures used for this project are based on work previously reported by Wilmsmeyer et al.[10,11] Experiments were performed in an UHV chamber with a base pressure of 10^{-9} Torr. These low pressures are necessary to minimize the possibility of surface contamination on the silica sample, which is a highly effective sorbent especially at cryogenic temperatures. Control experiments were performed to ensure that background water and other common UHV contaminants did not adsorb to the surface over the duration of a typical experiment. Specifically, infrared spectroscopic measurements showed no sign of changes to the silica sample (either in spectral regions assigned to OH or CH stretches) over several hours in a vacuum with the surface at a temperature of 130 K. The total coverage of contaminants in this work remains low, largely due to the very high surface area of our particles, which necessitates very long exposure times to accumulate even trace levels of contamination in an UHV environment.

Silica samples were prepared in a hydraulic press by packing approximately 5 mg of Aerosil (200 m^2/g surface area, 12 nm mean particle diameter) into a 50 μm thick tungsten mesh grid (Tech Etch). The mesh was mounted to a McAllister X-Y-Z manipulator via nickel clamps and 5 mm thick copper leads connected to an external power supply to achieve precise control of sample position and temperature. Sample temperature was monitored with a type-K thermocouple spot-welded to the mesh immediately adjacent to the silica sample. The mesh was heated resistively using a custom external power supply. The power leads and thermocouple wire pass through a tube in the manipulator, which could be filled with liquid nitrogen to cool the silica sample to cryogenic temperatures. Prior to each experiment, the silica sample was pretreated by heating to 700 K for 5 min, which removes possible trace surface contamination. Pretreatment also significantly dehydroxylates the surface such that it is dominated by isolated OH groups at an approximate density of ∼2 OH/nm^2.[12−16] After heating, the sample was cooled to cryogenic temperatures to maximize uptake during dosing.

Dosing. 2-CEES, diethyl sulfide, chloroethane, 1-chloropropane, 1-chlorobutane, and 1-chloropentane (molecular structures are provided in Figure 1) were purchased from Sigma-Aldrich and transferred to stainless steel cylinders mounted on a gas-handling manifold configured with VCR seals and fittings. Each chemical was purified with two or more freeze−pump−thaw cycles immediately prior to use. All compounds employed for this work are liquids at room temperature but have sufficiently high vapor pressures to deliver gas-phase molecules

DOI: 10.1021/jp509516x
J. Phys. Chem. C 2015, 119, 365−372

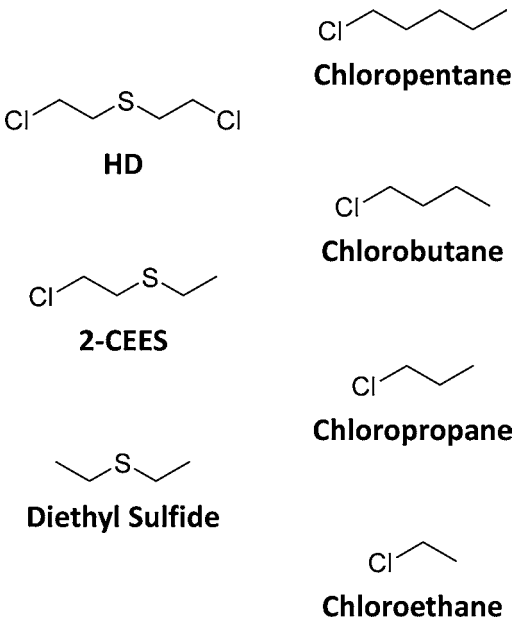

Figure 1. Schematics for HD and molecules explored in this work.

to the UHV chamber through a directional capillary array doser positioned approximately 5 mm from the silica surface. The doser was mounted on a translation stage and retracted when not in use. The manifold was kept under vacuum at all times except during dosing to minimize contamination and was vacuum-heated for 12 h at over 500 K to clean the system between experiments with each molecule. The temperature of the silica sample during dosing was adjusted for each molecule to attain high (at least 75%) surface coverage within 3−7 min.

Infrared Spectroscopy. The silica sample was monitored with transmission Fourier-transform infrared spectroscopy (FTIR) before, during, and after dosing to identify adsorbed molecules and changes in surface vibrational modes. The IR spectra were recorded using a Nicolet Nexus 670 FTIR spectrometer integrated with the UHV chamber. All IR spectra consist of 128 scans recorded at 4 cm^{-1} resolution. IR spectra of clean silica employed an empty spot on the mesh as the reference background. Spectra of species adsorbed on the silica sample employed a spectrum of the clean silica as a reference.

Annealing. Previous work indicates that effective TPD measurements require a homogeneous distribution of adsorbed molecules throughout the particulate sample.[17] We achieved this distribution by annealing the silica sample immediately after dosing to a sufficiently high temperature for the adsorbed molecules to diffuse evenly through the packed bed of particles. A different anneal temperature was chosen for each molecule to reduce the surface concentration to submonolayer coverage and achieve uniform distributions. Anneal temperatures were 219 K for 2-CEES, 198 K for diethyl sulfide, 163 K for chloropropane, 181 K for chlorobutane, and 193 K for chloropentane. Chloroethane did not require annealing to remove multilayers and achieve a uniform distribution on the surface. Surface coverage for all molecules was controlled by varying the annealing duration. After annealing, the samples were rapidly cooled to well below their desorption temperatures, where the TPD measurements were initiated. Sufficient annealing can be confirmed experimentally by comparing plots of desorption rate vs temperature at different experimental coverages. Nonuniform surface coverage is evidenced by poor alignment of the trailing, high-temperature edges of the TPD distributions.[17]

Temperature-Programmed Desorption. TPD experiments were performed by heating the sample and detecting desorbed species with a doubly differentially pumped, axially mounted quadrupole mass spectrometer (Extrel) tuned to the most abundant mass fragments for each molecule. The mass spectrometer views a 0.35 cm^2 spot on the sample with an acceptance angle of ±0.4° such that the signal from molecules that may desorb from the sample holder is minimized. The heating rate for the TPD measurements was maintained at 0.2 K/s with a proportional-integral-derivative controller (Honeywell) and custom power supply.

3. RESULTS

Infrared Studies of Adsorption. Previous studies of 2-CEES and other polar compounds demonstrated the use of infrared spectroscopy in the characterization of interactions between silica and adsorbed molecules.[4,5] Figure 2 shows a

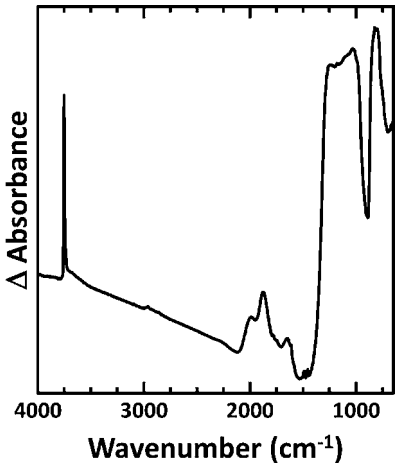

Figure 2. Infrared spectrum of a clean silica sample following pretreatment at 700 K for 5 min (see the text).

spectrum of clean silica immediately before exposure to the adsorbate. The sharp absorption feature at 3750 cm^{-1} is characteristic of free surface silanol groups.[18] The shoulder at 3700 cm^{-1} is indicative of geminal silanols, but the small size of this band relative to the main peak indicates that isolated silanols dominate the surface.[12−15,19] This is consistent with a study that measured the distributions of free, geminal, and hydrogen-bonded OH surface groups per unit area as a function of temperature from 473 to 1473 K.[16] The wavenumber region from 1400 to 650 cm^{-1} is dominated by bulk infrared modes of silica that obscure several adsorbate bands (see below), including those associated with the scissor mode for CH_2 adjacent to Cl (1215 cm^{-1}) and the C−Cl stretch (600−800 cm^{-1}) for some of the molecules used in this work.

IR difference spectra following uptake of chlorobutane, diethyl sulfide, and 2-CEES on silica are presented in Figure 3A. Figure 3B shows IR difference spectra for the silica particles following uptake of the aliphatic chloroalkanes. The inverted feature at 3750 cm^{-1} is the result of a shift in that band as the surface silanol groups transform from free SiOH to hydrogen-bonded groups. With the assumption that the absorbance intensity of the free OH band is directly proportional to the

DOI: 10.1021/jp509516x
J. Phys. Chem. C 2015, 119, 365−372

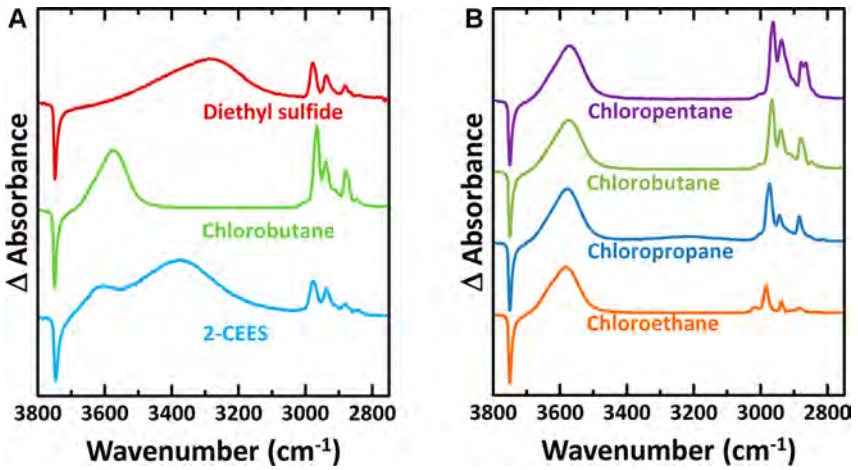

Figure 3. (A) Infrared spectra of adsorbed diethyl sulfide (top, red), chlorobutane (middle, green), and 2-CEES (bottom, blue) on silica. The spectra are normalized to the integrated area of the free OH band such that the spectra represent equivalent effective SiOH occupation fractions, θ (see the text). (B) Infrared spectra of adsorbed chloroalkanes.

surface concentration of free OH, the decrease in intensity of the feature at 3750 cm^{-1} following exposure to the gas of interest is used to determine the fraction of silanol groups involved in hydrogen bonding. In this study, surface coverage, θ, is reported in terms of the fraction of silanol groups bound to an adsorbate; for example, $\theta = 1$ represents occupation of all hydrogen-bonding sites. The monotonic profile and excellent alignment of the TPD curves shown in Figure 4 are evidence

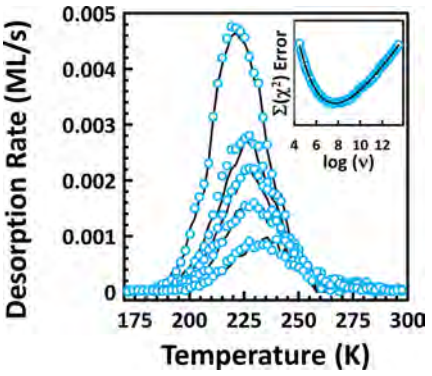

Figure 4. Experimental (blue circles) and simulated (black lines) TPD curves for 2-CEES at different coverages. From top to bottom: θ = 0.79, 0.46, 0.32, 0.21, and 0.17. The inset shows a 6th-order polynomial fit to χ^2 error values between simulated and experimental data used to determine the best prefactor value.

for the absence of significant multilayers. Furthermore, the decrease in IR signal from hydrogen-bonded silanol groups during desorption directly correlates with a decrease in adsorbate IR bands and a rise in mass spectrometer (MS) signal at the parent molecular mass. This correlation is evidence that the adsorbed molecules are bound through the SiOH groups.

The large shift in the silanol absorption band, clearly evident in Figures 3 and 5, indicates that hydrogen bonds are an important driving force in the uptake of these molecules. Three key characteristics of the IR band for the SiO−H stretch stand out in the spectra for adsorbed molecules: (1) the SiO−H stretch band shifts to lower wavenumber (red-shift), (2) the hydrogen-bonded OH band has a much larger intensity than the free OH band, and (3) this band broadens significantly

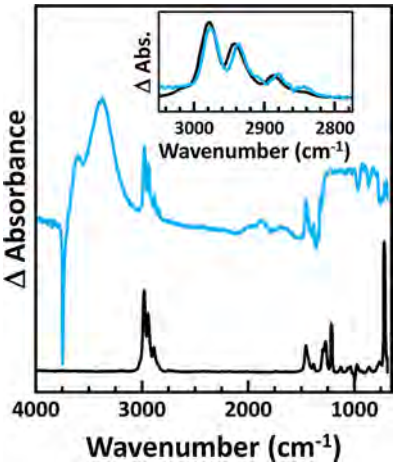

Figure 5. Infrared spectra of gas-phase 2-CEES (black) and 2-CEES adsorbed on silica (blue). The inset displays IR bands corresponding to methyl and methylene stretching modes.

upon adsorption. The red-shift is due to charge transfer as the hydrogen-bond acceptor donates electron density to SiOH. Upon hydrogen-bond formation, π electrons from the hydrogen-bond acceptor interact with the σ^* antibonding orbital on the silanol, thereby weakening the O−H bond and adding significant anharmonicity to the stretching mode.[20,21] The increase in peak intensity is due to the greater oscillator strength of hydrogen-bonded donor stretches.[22] Finally, the band broadening occurs because of the inhomogeneity in the configuration of the hydrogen-bonded molecules, which affects the strength and anharmonicity of each bond in different ways. Furthermore, coupling to other modes may reduce the lifetime of the O−H vibration, which increases the homogeneous band broadening.[23−26]

The bands near 3000 cm^{-1} are assigned to symmetric and asymmetric alkane stretching modes corresponding to molecules on the surface. A comparison of methylene stretching modes for each adsorbed molecule to corresponding gas-phase modes for the same molecule provides insight into the adsorption mechanism. Figure 5 shows spectra of 2-CEES adsorbed on silica and in the gas phase. The relative integrated areas of each band are similar, which indicates molecular

DOI: 10.1021/jp509516x
J. Phys. Chem. C 2015, 119, 365−372

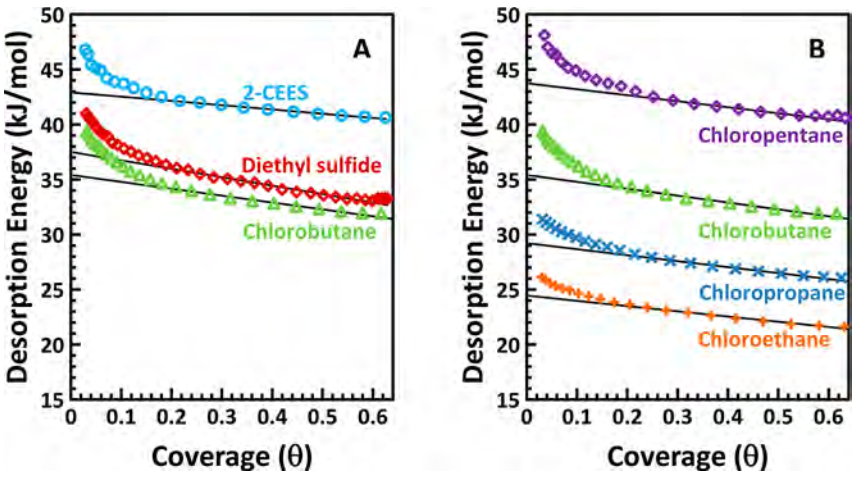

Figure 6. (A) $E_d(\theta)$ curves for the desorption of 2-CEES, diethyl sulfide, and chlorobutane from partially hydroxylated silica. (B) $E_d(\theta)$ curves for the desorption of four chloroalkanes from partially hydroxylated silica.

adsorption without subsequent decomposition or reaction. However, the bands assigned to $\nu_a(CH_2)$ and $\nu_s(CH_3)$ shift upon adsorption by 5 and 10 cm^{-1}, respectively, compared to the same modes in the gas phase. Similar shifts are observed in all molecules investigated here. They are likely due to dispersion interactions with the surface, restricted molecular degrees of freedom for the adsorbates, and changes in the CH_2 bending modes (the first overtone is in Fermi resonance with the CH_2 stretches). Unfortunately, the CH_2 bending modes could not be detected in the present work due to obstruction by the high absorbance of silica.

Temperature-Programmed Desorption. The desorption energies were determined by using TPD. After dosing and annealing, the silica sample was heated at a constant rate of 0.2 K/s. This rate was chosen to allow adsorbed molecules sufficient time to diffuse throughout the pressed sample before desorbing. The mass spectrometer, tuned to mass fragments unique to the desorbing molecule, tracked changes in the gas-phase number density of the analytes as a function of surface temperature. The raw signal was then multiplied by $T^{1/2}$ to correct for the velocity-dependent detection probability that affects line-of-sight, differentially pumped, mass spectrometric TPD measurements.[27] The resulting distribution was directly proportional to desorption rate. Molecular desorption, as opposed to decomposition on the surface and subsequent desorption of products, was confirmed by comparing the fragmentation pattern for the pure gases to that recorded during desorption. The desorption rates for 2-CEES at different initial coverages are shown in Figure 4.

The variation of the desorption rate with the initial coverage provides a qualitative understanding of bonding. The alignment of the trailing edges indicates that adsorbed molecules have sufficient mobility to diffuse to the strongest available adsorption sites during the temperature ramp prior to desorption.[17] The maximum in the desorption rate shifts to higher temperatures with lower coverage. This is evidence that the residence time and binding is governed by molecule–surface, rather than molecule–molecule, forces.

Quantitative interpretation of TPD spectra is based on the Polanyi–Wigner relationship (eq 1), which can be rewritten as eq 2 to express desorption energy as a function of coverage. The experimental TPD data were analyzed by using the inverted Polanyi–Wigner equation to determine the desorption energy at each temperature and corresponding coverage according to the methods outlined by others[17] and recently used to study the desorption energetics of molecules from particulate silica.[10,11] The desorption energies are then plotted as a function of coverage and modeled with first-order kinetics. Numerical integration of the desorption energy (E_d) vs coverage (θ) curve obtained from the highest experimental coverage gives simulated TPD curves for any desired initial coverage lower than that highest experimental coverage. The prefactor (ν in eq 1) is assumed to be independent of coverage and temperature for this type of analysis and is used as a fitting parameter to maximize agreement between simulated and experimental desorption rate curves. Specifically, the prefactor is adjusted to minimize the sum of the squared residuals between experimental data and simulated data at each coverage. Figure 4 shows simulated data (black lines) obtained with an optimized prefactor plotted over the experimental E_d vs temperature data for five initial coverages. The inset shows the SSR plot used to optimize the prefactor.

$$-\frac{d\Theta}{dt}(\Theta, T_S) = \upsilon(\Theta, T_S)\exp[-E_d(\Theta)/k_B T_S]\Theta^n \quad (1)$$

$$E_d(\Theta) = -k_B T_S \ln\left(-\frac{d\Theta/dt}{\upsilon\Theta}\right) \quad (2)$$

After optimizing the Polanyi–Wigner prefactor, the reported desorption energy is determined from the plot of desorption energy vs coverage (Figure 6A). The curvature in this plot is likely due to a nonuniformity of the silica surface. Some silanol sites, defect sites in particular, likely contribute higher binding energy sites to the surface. Furthermore, hydrogen bonding, though the most significant force in the physisorption of these molecules, is not the only type of interaction that determines the overall binding energy. Other surface–adsorbate interactions, including dispersion forces, can significantly affect the activation energy for desorption. Thus, the local variations in silanol density likely affect the desorption energy for individual molecules. In this study, our focus is on the desorption energy of a single adsorbate on a defect-free region of the silica surface; therefore, the linear portion of the E_d curve is extrapolated to zero coverage. Desorption energy distributions for 2-CEES, diethyl sulfide, and chlorobutane are presented in Figure 6A. Figure 6B contains desorption energy distributions for the

DOI: 10.1021/jp509516x
J. Phys. Chem. C 2015, 119, 365–372

chloroalkanes. The extrapolated, zero-coverage limit desorption energies for each of the molecules studied are presented in Table 1.

Table 1. Desorption Energies and Pre-Exponential Factors for Molecules Tested in This Study[a]

molecule	E_d (±2.3 kJ/mol)	log(ν) (±0.6)
2-CEES	42.9	7.7
diethyl sulfide	37.5	6.5
chloropentane	43.7	9.1
chlorobutane	35.4	7.3
chloropropane	29.2	6.3
chloroethane	24.4	5.9

[a]Error values are ± one standard deviation calculated from three independent TPD experiments.

4. DISCUSSION

We have explored the fundamental nature of gas−surface hydrogen-bond formation between simulant molecules (2-CEES, diethyl sulfide, and chlorobutane) and partially hydroxylated silica to help construct an understanding of how sulfur mustard gas adheres to hydroxyl-containing surfaces. In this study, infrared spectroscopy was employed to probe the extent of charge transfer, a key mechanistic step in hydrogen-bond formation, from the adsorbate to the hydroxyl group of a well-characterized silica surface. The overall strengths of the hydrogen bonds were gauged by performing TPD measurements to determine the activation energy for desorption. Together, these techniques provide insight into the roles that dipole−dipole interactions, charge transfer, and dispersion forces play in the uptake of mustard on polar surfaces.

2-CEES−Silica Hydrogen-Bond Formation. 2-CEES uptake on silica is primarily driven by the formation of hydrogen bonds with surface hydroxyl groups. These hydrogen-bonding interactions are evidenced in the IR spectra of adsorbed 2-CEES (Figure 5), which clearly show the reduction of the band associated with free surface hydroxyl groups (reduced absorbance at 3750 cm^{-1}) as two new broad IR features, signatures of hydrogen bonding, emerge. The two broad but distinct IR absorbance features at 3598 and 3359 cm^{-1} are in the infrared spectral range associated with surface SiO−H stretches but are red-shifted significantly from the free silanol band. This red-shift reflects a decrease in the SiO−H vibrational energy caused by charge transfer from the hydrogen-bond acceptor to the antibonding orbital of the SiO−H bond.[8,28] In this way, infrared spectroscopic measurement of the SiO−H vibrational frequency is a probe of the extent of charge transfer in gas−surface hydrogen-bond formation and reveals two distinct types of charge donors (lone-pair hydrogen-bond acceptors) within 2-CEES.

The chlorine and sulfur moieties within the 2-CEES molecule are both potential hydrogen-bond acceptor sites. Therefore, we have studied the uptake of chlorobutane and diethyl sulfide to help identify the contributions from each site. Spectra for adsorbed chlorobutane show a strong absorbance feature at 3571 cm^{-1}, which is due to excitation of the SiO−H stretch associated with the Cl···H−OSi hydrogen bond. Diethyl sulfide also forms hydrogen bonds with the surface, but the band associated with the SiO−H stretch is much further red-shifted in the IR spectra. This band appears at 3280 cm^{-1}. Thus, we assign the 3598 and 3359 cm^{-1} absorption features in the IR spectra of adsorbed 2-CEES to Cl···H−OSi and S···H−OSi hydrogen bonds, respectively, in agreement with a previous study.[4]

The infrared spectral assignments reveal that the extent of charge transfer during uptake and hydrogen-bond formation is greater for molecules that bind through the sulfur than through the chlorine constituents of the molecule and that both types of interactions occur for 2-CEES. However, the extent of charge transfer does not always correlate with the strength of the hydrogen bond. Electrostatic interactions also play a major role in hydrogen-bond formation, and further measurements are necessary to assess the relative contribution of each type of hydrogen bond to the overall adsorption process. Therefore, we have performed a series of TPD studies to help determine the overall energy required to rupture the hydrogen bonds and drive the molecules from the surface.

Charge Transfer and Electrostatic Interactions. Previous studies in solution, in the gas phase, and at the gas−surface interface reveal a positive, linear correlation between $\Delta\nu$ (the shift in the frequency for the O−H stretch of a hydrogen bond) and intermolecular hydrogen-bond strength for electronically similar moieties.[10,11,29−33] On the basis of this previous work alone, one would infer that the larger $\Delta\nu$ in spectra of adsorbed diethyl sulfide ($\Delta\nu$ = 485 cm^{-1}) compared to chlorobutane ($\Delta\nu$ = 190 cm^{-1}) is indicative of a stronger hydrogen bond. However, as described above, electrostatic (in this case, dipole−dipole) interactions also play a role in hydrogen-bond forces. Calculations indicate that the molecular dipole moments for chlorobutane and diethyl sulfide are 2.47 and 1.68 D, respectively.[34] Thus, on the basis of the magnitude of the dipoles, one might predict that chlorobutane would form a stronger hydrogen bond with silanol than diethyl sulfide. This is contrary to the conclusion based solely on the extent of the red-shift in the SiO−H vibrational frequency in the hydrogen-bonded complexes.

The interplay between dipole−dipole interactions and charge transfer has been explored in a recent computational study on hydrogen bonding of dimethyl sulfide and chloromethane to gas-phase water (among a variety of other species).[8] In that study, $\Delta\nu$ for the O−H stretch was 125 cm^{-1} larger for water bound to dimethyl sulfide than for water bound to chloromethane. However, the calculated hydrogen-bond strengths for both molecules were similar relative to other molecules studied in that work. Analysis of our TPD measurements for diethyl sulfide and chlorobutane (See Figure 6A and Table 1) is consistent with these calculations. That is, the activation energies for desorption for diethyl sulfide and chlorobutane from silica were found to be nearly the same within the error bars for these measurements (37.5 ± 2.3 and 35.4 ± 2.3 kJ/mol). Thus, we conclude that differences in the charge transfer contribution are balanced by other intermolecular forces, such as dipole−dipole interactions, to yield similar activation energies for desorption. Therefore, in the case of 2-CEES adsorption, hydrogen-bond formation through the sulfur or the chlorine component likely leads to very similar binding strengths (similar to those of diethyl sulfide and chlorobutane) for isolated 1:1 type interactions. However, if 2-CEES were to interact simultaneously with an SiOH group through the chlorine and another SiOH group through the sulfur, then the activation energy for desorption may be much higher.

2-CEES Adsorption Mechanism. We have investigated whether each adsorbed 2-CEES molecule interacts with a single silanol group (1:1 adsorbate:silanol ratio) or two adjacent

DOI: 10.1021/jp509516x
J. Phys. Chem. C 2015, 119, 365−372

silanol groups (1:2 ratio). As described above, the surface hydroxyl density on silica pretreated to 700 K is estimated to be ~2 OH/nm^2, which corresponds to an approximate spacing of 0.7 nm between silanols.[3,16,35] This spacing is likely sufficient to allow the two polar functional groups in 2-CEES, separated by an ethyl chain, to simultaneously bind to adjacent hydroxyls. However, analysis of the relative surface coverages for 2-CEES and diethyl sulfide at identical SiOH occupation densities suggests that 2-CEES adsorbs similarly to diethyl sulfide; that is, there is only one molecule−surface hydrogen bond per adsorbed molecule. More specifically, the spectra presented in Figure 3A are normalized such that they represent the same number of occupied SiOH surface sites. At this coverage, we find that the integrated areas under the bands for the CH_2 asymmetric stretching mode of each molecule are nearly identical, strongly suggesting that the adsorbate-to-SiOH ratios (necessarily 1:1 for diethyl sulfide) are the same. This conclusion is supported by the TPD data, which indicates that the desorption energy for 2-CEES is only 15% greater than that of diethyl sulfide, as opposed to the much larger energy increase one might expect if two hydrogen bonds were formed per molecule.

Stabilization from Secondary Interactions. The slightly higher desorption energy for 2-CEES compared to those of chlorobutane or diethyl sulfide is likely due to surface−adsorbate interactions other than the hydrogen bonds. Weaker secondary interactions likely play a role in controlling the activation energy for desorption. Previous work reported a binding energy increase of 7 kJ/mol per additional methylene for a series of linear hydrocarbons on MgO(100).[36] We have observed a similar trend on amorphous silica. Figure 6A shows the coverage-dependent desorption energies for a series of linear chloroalkanes that differ only by alkane chain length. As with 2-CEES, diethyl sulfide, and chlorobutane, the desorption energy is largely invariant with coverage, except for the lowest coverages due to a small concentration of sites that lead to unusually high binding energies. The linear portions of the $E_d(\theta)$ distributions are extrapolated to the zero coverage limit and the values are provided in Table 1. The chloroalkane desorption energies range from 24 kJ/mol for the shortest chain molecule studied to 44 kJ/mol for the longest chain molecule. Each methylene group contributes 5−8 kJ/mol to the overall desorption energy. It is unlikely that this energy difference is caused by changes to the SiO−H···Cl hydrogen-bond strength, because the fundamental nature of the hydrogen bonds, as gauged by the SiO−H stretching frequency ($\Delta\nu$ = 180 cm^{-1} for all four molecules), appears to be identical (see Figure 3B). Furthermore, calculations indicate that the magnitude of the dipoles for the chloroalkanes are not strongly dependent on chain length. The permanent dipole moments range from 2.3 D for chloroethane to 2.5 D for chloropentane.[34] Thus, the measured increase in desorption energy as a function of chain length likely arises from surface−adsorbate dispersion interactions. On the basis of these results, we reason that similar dispersion interactions for the larger 2-CEES molecule, relative to diethyl sulfide and chlorobutane, account for the differences in the desorption energies for these molecules. Finally, we note that, in addition to the desorption energy, the Polanyi−Wigner pre-exponential factors (ν) for this series of chloroalkanes depend on chain length. This phenomenon is well-known from other work[36] and is likely due to the increased entropic penalty of constraining larger molecules to a surface as well as differences in the diffusivity of the molecules through the silica particles.[36]

5. SUMMARY

We have found that the uptake of 2-CEES on silica is driven primarily by the formation of hydrogen bonds to the thioether and chloro moieties. Although both types of hydrogen bonds have similar overall strength, the contributions to bond strength from other forces, including charge transfer, are apparently different. The S···H−OSi bond has a larger charge transfer contribution, whereas the Cl···H−OSi bond has a larger contribution from other intermolecular forces. Dispersion forces between the hydrocarbon segments of the adsorbed molecules and surface atoms provide additional stabilization. Each adsorbed 2-CEES molecule occupies a single silanol group, even though the sulfur and chlorine atoms have sufficient spacing to span adjacent silanol groups. The 1:1 bonding motif may be a result of a significant entropic penalty that would be required for dual hydrogen-bond formation.

A major motivation of this work was to develop insight into the desorption energetics and binding mechanisms for the chemical warfare agent HD on the surface of an environmentally relevant hydroxylated material. HD has the same molecular structure as 2-CEES except for the addition of a terminal chlorine atom; therefore, it is likely that HD and 2-CEES have similar binding mechanisms and desorption energies. The extra heteroatom may increase desorption energy somewhat due to added surface−adsorbate dispersion interactions, but this will be highly dependent on the geometry of the adsorbed molecules and degree of silica hydroxylation. Notwithstanding, we predict that the overall desorption energy for HD from silica will be within several kilojoules per mole of the values reported here for its closest simulant, 2-CEES.

AUTHOR INFORMATION

Corresponding Author

*E-mail: jrmorris@vt.edu.

Notes

The authors declare no competing financial interest.

ACKNOWLEDGMENTS

We are grateful to the Army Research Office (W911NF-09-1-0150) and the Defense Threat Reduction Agency (W911NF-06-1-0111) for providing support. We thank Advanced Research Computing at Virginia Tech for providing computational resources and technical support that have aided in the research reported in this paper. We also thank Dr. Frank A. Weinhold for helpful discussions about hydrogen bonding on silica.

REFERENCES

(1) Tucker, J. B. *War of Nerves: Chemical Warfare From World War I to Al-Qaeda*; Pantheon Books: New York, 2006.

(2) OPCW. *Convention on the Prohibition of the Development, Production, Stockpiling and Use of Chemical Weapons and on Their Destruction*; Technical Secretariat of the Organisation for the Prohibition of Chemical Weapons: The Hague, 2005.

(3) Brevett, C. A. S.; Sumpter, K. B.; Wagner, G. W.; Rice, J. S. Degradation of the Blister Agent Sulfur Mustard, Bis(2-chloroethyl) Sulfide, on Concrete. *J. Hazard. Mater.* **2007**, *140*, 353−360.

(4) Panayotov, D.; Yates, J. T. Bifunctional Hydrogen Bonding of 2-Chloroethyl Ethyl Sulfide on TiO_2−SiO_2 Powders. *J. Phys. Chem. B* **2003**, *107*, 10560−10564.

DOI: 10.1021/jp509516x
J. Phys. Chem. C 2015, 119, 365−372

(5) Panayotov, D. A.; Paul, D. K.; Yates, J. T. Photocatalytic Oxidation of 2-Chloroethyl Ethyl Sulfide on TiO_2−SiO_2 Powders. *J. Phys. Chem. B* **2003**, *107*, 10571−10575.
(6) Thompson, T. L.; Panayotov, D. A.; Yates, J. T. Adsorption and Thermal Decomposition of 2-chloroethyl Ethyl Sulfide on TiO_2 Surfaces. *J. Phys. Chem. B* **2004**, *108*, 16825−16833.
(7) Thompson, T. L.; Panayotov, D. A.; Yates, J. T.; Martyanov, I.; Klabunde, K. Photodecomposition of Adsorbed 2-Chloroethyl Ethyl Sulfide on TiO_2: Involvement of Lattice Oxygen. *J. Phys. Chem. B* **2004**, *108*, 17857−17865.
(8) Freindorf, M.; Kraka, E.; Cremer, D. A Comprehensive Analysis of Hydrogen Bond Interactions Based on Local Vibrational Modes. *Int. J. Quantum Chem.* **2012**, *112*, 3174−3187.
(9) Weinhold, F.; Klein, R. A. What Is a Hydrogen Bond? Mutually Consistent Theoretical and Experimental Criteria for Characterizing H-Bonding Interactions. *Mol. Phys.* **2012**, *110*, 565−579.
(10) Wilmsmeyer, A. R.; Gordon, W. O.; Davis, E. D.; Troya, D.; Mantooth, B. A.; Lalain, T. A.; Morris, J. R. Infrared Spectra and Binding Energies of Chemical Warfare Nerve Agent Simulants on the Surface of Amorphous Silica. *J. Phys. Chem. C* **2013**, *117*, 15685−15697.
(11) Wilmsmeyer, A. R.; Uzarski, J.; Barrie, P. J.; Morris, J. R. Interactions and Binding Energies of Dimethyl Methylphosphonate and Dimethyl Chlorophosphate with Amorphous Silica. *Langmuir* **2012**, *28*, 10962−10967.
(12) Dijkstra, T. W.; Duchateau, R.; van Santen, R. A.; Meetsma, A.; Yap, G. P. A. Silsesquioxane Models for Geminal Silica Surface Silanol Sites. A Spectroscopic Investigation of Different Types of Silanols. *J. Am. Chem. Soc.* **2002**, *124*, 9856−9864.
(13) Ghiotti, G.; Garrone, E.; Morterra, C.; Boccuzzi, F. Infrared Study of Low Temperature Adsorption. 1. Carbon Monoxide on Aerosil. An Interpretation of the Hydrated Silica Spectrum. *J. Phys. Chem.* **1979**, *83*, 2863−2869.
(14) Hoffmann, P.; Knözinger, E. Novel Aspects of Mid and Far IR Fourier Spectroscopy Applied to Surface and Adsorption Studies on SiO_2. *Surf. Sci.* **1987**, *188*, 181−198.
(15) Van Roosmalen, A. J.; Mol, J. C. An Infrared Study of the Silica Gel Surface. 1. Dry Silica Gel. *J. Phys. Chem.* **1978**, *82*, 2748−2751.
(16) Zhuravlev, L. T. The Surface Chemistry of Amorphous Silica. Zhuravlev Model. *Colloids Surf., A* **2000**, *173*, 1−38.
(17) Zubkov, T.; Smith, R. S.; Engstrom, T. R.; Kay, B. D. Adsorption, Desorption, and Diffusion of Nitrogen in a Model Nanoporous Material. II. Diffusion Limited Kinetics in Amorphous Solid Water. *J. Chem. Phys.* **2007**, *127*, 184708.
(18) McDonald, R. S. Surface Functionality of Amorphous Silica by Infrared Spectroscopy. *J. Phys. Chem.* **1958**, *62*, 1168−1178.
(19) Takei, T.; Kato, K.; Meguro, A.; Chikazawa, M. Infrared Spectra of Geminal and Novel Triple Hydroxyl Groups on Silica Surface. *Colloids Surf., A* **1999**, *150*, 77−84.
(20) Tsyganenko, A. A.; Babaeva, M. A. Infrared Spectrum of Ammonia Adsorbed by Si−OH Groups on a Silica Surface. *Opt. Spectrosc.* **1983**, *54*, 665−666.
(21) Civalleri, B.; Ugliengo, P. First Principles Calculations of the Adsorption of NH_3 on a Periodic Model of the Silica Surface. *J. Phys. Chem. B* **2000**, *104*, 9491−9499.
(22) Tsubomura, H. Nature of the Hydrogen Bond. III. The Measurement of the Infrared Absorption Intensities of Free and Hydrogen-Bonded OH Bands. Theory of the Increase of the Intensity Due to the Hydrogen Bond. *J. Chem. Phys.* **1956**, *24*, 927−931.
(23) Kjaergaard, H. G.; Garden, A. L.; Chaban, G. M.; Gerber, R. B.; Matthews, D. A.; Stanton, J. F. Calculation of Vibrational Transition Frequencies and Intensities in Water Dimer: Comparison of Different Vibrational Approaches. *J. Phys. Chem. A* **2008**, *112*, 4324−4335.
(24) Takahashi, K. Theoretical Study on the Effect of Intramolecular Hydrogen Bonding on OH Stretching Overtone Decay Lifetime of Ethylene Glycol, 1,3-Propanediol, and 1,4-Butanediol. *Phys. Chem. Chem. Phys.* **2010**, *12*, 13950−13961.
(25) Morita, M.; Takahashi, K. Theoretical Study on the Difference of OH Vibrational Spectra Between OH-$(H_2O)(3)$ and OH-$(H_2O)(4)$. *Phys. Chem. Chem. Phys.* **2012**, *14*, 2797−2808.
(26) Petkovic, M. O−H Stretch in Phenol and Its Hydrogen-Bonded Complexes: Band Position and Relaxation Pathways. *J. Phys. Chem. A* **2012**, *116*, 364−371.
(27) Daschbach, J. L.; Kim, J.; Ayotte, P.; Smith, R. S.; Kay, B. D. Adsorption and Desorption of HCl on Pt(111). *J. Phys. Chem. B* **2005**, *109*, 15506−15514.
(28) Ramesh, S. G.; Re, S.; Hynes, J. T. Charge Transfer and OH Vibrational Frequency Red Shifts in Nitrate−Water Clusters. *J. Phys. Chem. A* **2008**, *112*, 3391−3398.
(29) Badger, R. M. A Relation between Internuclear Distances and Bond Force Constants. *J. Chem. Phys.* **1934**, *2*, 128−131.
(30) Badger, R. M.; Bauer, S. H. Spectroscopic Studies of the Hydrogen Bond. II. The Shift of the O−H Vibrational Frequency in the Formation of the Hydrogen Bond. *J. Chem. Phys.* **1937**, *5*, 839−851.
(31) Cioslowski, J.; Liu, G. H.; Castro, R. A. M. Badger's Rule Revisited. *Chem. Phys. Lett.* **2000**, *331*, 497−501.
(32) Joshi, R.; Ghanty, T. K.; Mukherjee, T. Substituent Effect on Ionization Potential, O−H Bond Dissociation Energy and Intra-Molecular Hydrogen Bonding in Salicylic Acid Derivatives. *J. Mol. Struct.* **2010**, *948*, 47−54.
(33) Rivera-Rivera, L. A.; McElmurry, B. A.; Scott, K. W.; Lucchese, R. R.; Bevan, J. W. The Badger−Bauer Rule Revisited: Correlation of Proper Blue Frequency Shifts in the OC Hydrogen Acceptor with Morphed Hydrogen Bond Dissociation Energies in OC−HX (X = F, Cl, Br, I, CN, CCH). *J. Phys. Chem. A* **2013**, *117*, 8477−83.
(34) Edwards, A. Gaussian Calculations Performed Using Gaussian 09 Package at the B97D/6-316** level. 2014.
(35) Rimola, A.; Costa, D.; Sodupe, M.; Lambert, J.-F.; Ugliengo, P. Silica Surface Features and Their Role in the Adsorption of Biomolecules: Computational Modeling and Experiments. *Chem. Rev.* **2013**, *113*, 4216−4313.
(36) Tait, S. L.; Dohnalek, Z.; Campbell, C. T.; Kay, B. D. *n*-Alkanes on MgO(100). II. Chain Length Dependence of Kinetic Desorption Parameters for Small *n*-Alkanes. *J. Chem. Phys.* **2005**, *122*.

DOI: 10.1021/jp509516x
J. Phys. Chem. C 2015, 119, 365−372